Morphology and Mechanical Properties of Crystalline Polymers. 4. Behavior of Spherulites in Polyethylene Subjected to Biaxial Tension or Pure Shear

T. T. Wang

AT&T Bell Laboratories, Murray Hill, New Jersey 07974

Received June 20, 1991; Revised Manuscript Received August 10, 1991

ABSTRACT: The elastic responses of spherulites, when the spherulitic polyethylene is subjected to biaxial tension or pure shear, are analyzed using the scheme developed previously in this series of investigations. In both types of loading, the stress and strain distributions are found to be highly nonuniform and tend to infinity at the spherulite centers. The singular behavior, which is also found in simple tension but not in hydrostatic tension or compression, is attributed to a combination of two factors, namely, the spherically symmetric structure of the spherulite and the lack of spherical symmetry in the applied load. The study further shows the region of stress concentration to be much more localized around the spherulite center in biaxial tension than in simple tension and pure shear; thus, the spherulitic polymer should be more prone to fracture under biaxial tension. Results of the analysis are found to be in good agreement with experimental data reported in the literature.

Introduction

In a previous publication,[1] we analyzed the local deformation of spherulites in spherulitic polyethylene when the polymer is subjected to simple (uniaxial) tension. It was shown that because of their spherically isotropic nature,[2] the spherulites develop a highly inhomogeneous state of stress and strain which tend to infinity at the centers. These predictions have been subsequently confirmed by Adams and Thomas[3] in their electron microscopic experiment. The spherical isotropy arises from the unique morphological structure of the spherulite[4-6] and can be characterized by five independent elastic moduli in reference to a spherical coordinate system having its origin at the center of the spherulite.[7] It was also shown[1] that the spherulites develop inhomogeneous deformation but not stress singularity when the polymer is subjected to hydrostatic (triaxial) tension or compression. These results suggest that the singular behavior found in simple tension does not arise in all types of loading and its occurrence may in fact depend on the symmetry nature of the applied load with respect to the center of spherulite. In view of this and the critical influence that the stress singularities could have on the ultimate strength of spherulitic polymers, we have carried out additional analysis of cases involving biaxial tension and pure shear. The results are compared with experimental data reported in the literature.

Analysis

As in the previous treatment of simple tension,[1] we make use of a composite model for analyzing the problems of biaxial tension and pure shear in spherulitic polyethylene. The model consists of a spherically shaped spherulite which, with the center of anisotropy at its geometrical center, is assumed to be embedded in a large, homogeneous matrix having the overall isotropic properties of the bulk polymer. Referring to Figure 1, we attach to the model a rectangular coordinate system (x, y, z) with its origin at the center of the spherulite. Since, in terms of applied loads, pure shear is equivalent to biaxial tension except for the fact that one of the biaxial loads is compressive,[8] it is convenient to treat both problems as a general case of biaxial loading in which one of the applied loads is directed along the z axis and the other along the x axis. This treatment has the added advantage in that the solutions to both biaxial tension and pure shear can be obtained by superposition of solutions to the simple tension problem.[1]

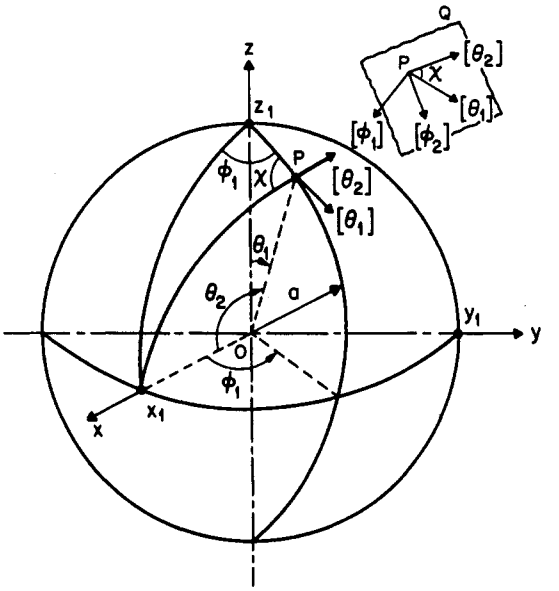

Figure 1. Sketch of spherulite in reference to two spherical coordinate systems (r_1, θ_1, ϕ_1) and (r_2, θ_2, ϕ_2) and their relations to each other. ϕ_2 is the angle between the z axis and the plane (Ox_1P). Plane Q is the tangent plane at point P. $[\theta_i]$ and $[\phi_i]$ $(i = 1, 2)$ are the directions of the corresponding coordinates axes θ_i and ϕ_i $(i = 1, 2)$. r_1 and r_2 $(r_1 = r_2)$ are the distances between the origin and the point of interest, P, in the spherulite.

To accomplish this, we further introduce two spherical coordinate systems and refer the stresses due to the first load, along the z axis, to the system (r_1, θ_1, ϕ_1) and those due to the second, along the x axis, to another system (r_2, θ_2, ϕ_2), as shown in Figure 1, ϕ_2 being the angle between the z axis and the plane (Ox_1P), r_1 and r_2 $(r_1 = r_2)$ being the distance from the origin to the point of interest, P, in the spherulite. We then combine the stresses due to both

* Present address: Department of Materials Science and Engineering, Rutgers University, Piscataway, NJ 08855.

0024-9297/92/2225-0933$03.00/0

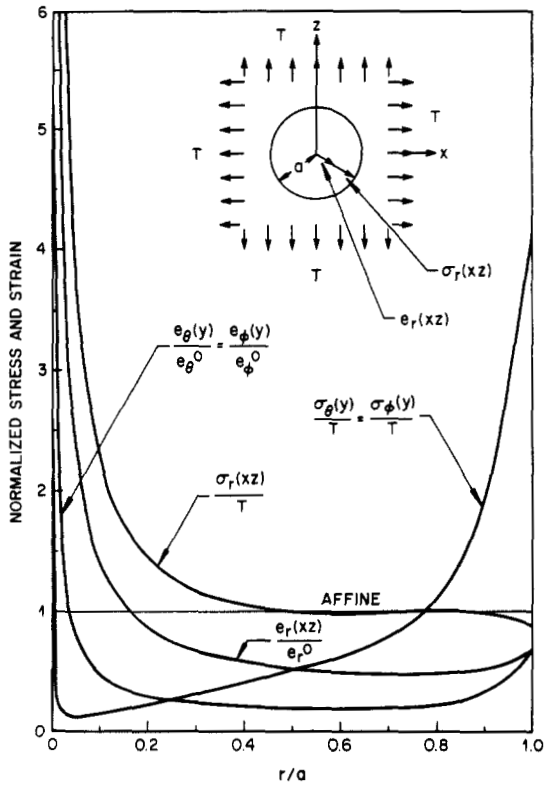

Figure 2. Distributions of major stresses and strains in the spherulite when the polymer is subjected to biaxial tension in the xz plane. Both stresses and strains have been normalized with the corresponding quantities at distant field and the radius, r, has been normalized with the outer radius, a, of the spherulite.

applied loads by referring them to the same coordinate system, say, (r_1, θ_1, ϕ_1). Since the two spherical coordinate systems are related to one another via the angle χ by

$$\cos\theta_2 = \sin\theta_1 \cos\phi_1$$

$$\cos\chi = -\cos\theta_1 \cos\phi_1/\sin\theta_2$$

$$\sin\chi = \sin\phi_1/\sin\theta_2 \tag{1}$$

if we denote the normal stresses, which are due to the second load and referred to the second coordinate system, by $\sigma_{r_2}^{(2)}$, $\sigma_{\theta_2}^{(2)}$, and $\sigma_{\phi_2}^{(2)}$, then the same stresses, when referred to the first coordinate system, are given by

$$\sigma_{r_1}^{(2)} = \sigma_{r_2}^{(2)}$$

$$\sigma_{\theta_1}^{(2)} = \sigma_{\theta_2}^{(2)} \cos^2\chi + \sigma_{\phi_2}^{(2)} \sin^2\chi$$

$$\sigma_{\phi_1}^{(2)} = \sigma_{\theta_2}^{(2)} \sin^2\chi + \sigma_{\phi_2}^{(2)} \cos^2\chi \tag{2}$$

Consequently, the total stresses σ_{r1}, $\sigma_{\theta 1}$, and $\sigma_{\phi 1}$ resulting from the combined action of two loads, when referred to the first coordinate system, are given by

$$\sigma_{r_1} = \sigma_{r_1}^{(1)} + \sigma_{r_1}^{(2)}$$

$$\sigma_{\theta_1} = \sigma_{\theta_1}^{(1)} + \sigma_{\theta_1}^{(2)} = \sigma_{\theta_1}^{(1)} + \sigma_{\theta_2}^{(2)} \cos^2\chi + \sigma_{\phi_2}^{(2)} \sin^2\chi$$

$$\sigma_{\phi_1} = \sigma_{\phi_1}^{(1)} + \sigma_{\phi_1}^{(2)} = \sigma_{\phi_1}^{(1)} + \sigma_{\theta_2}^{(2)} \sin^2\chi + \sigma_{\phi_2}^{(2)} \cos^2\chi \tag{3}$$

Biaxial Tension

The state of stress and strain under biaxial tension is obtained from the foregoing results by letting the loads along the x and z axes to be both tensile and of the same magnitude T. Since both loads lie in the xz plane, the stresses in this plane are of primary interest. Thus if we set $\phi_1 = \phi_2 = 0$ (which corresponds to the xz plane), we find from eq 1 $\chi = \pi$ and $\theta_1 = \theta_2 + \pi/2$. Application of these relations and the solutions of the simple tension problem (Appendix 1) to eqs 2 and 3 yields the stresses due to biaxial tension in the xz plane.

$$\sigma_{r_1}(xz) = 2A_{01}K_{01}\left[C_{33}\left(\nu_{01} - \frac{1}{2}\right) + 2C_{13}\right] r^{\nu_{01}-3/2} + \frac{1}{2}\sum_{m=1,3} A_{2m}\left[C_{33}K_{2m}\left(\nu_{2m} - \frac{1}{2}\right) + 2C_{13}(K_{2m} - 3)\right] r^{\nu_{2m}-3/2}$$

$$\sigma_{\theta_1}(xz) = 2A_{01}K_{01}\left[C_{11} + C_{12} + C_{13}\left(\nu_{01} - \frac{1}{2}\right)\right] r^{\nu_{01}-3/2} + \sum_{m=1,3} A_{2m}\left\{\frac{1}{2}K_{2m}\left[C_{11} + C_{12} + C_{13}\left(\nu_{2m} - \frac{1}{2}\right)\right] - 3C_{12}\right\} r^{\nu_{2m}-3/2}$$

$$\sigma_{\phi_1}(xz) = 2A_{01}K_{01}\left[C_{11} + C_{12} + C_{13}\left(\nu_{01} - \frac{1}{2}\right)\right] r^{\nu_{01}-3/2} + \sum_{m=1,3} A_{2m}\left\{\frac{1}{2}K_{2m}\left[C_{11} + C_{12} + C_{13}\left(\nu_{2m} - \frac{1}{2}\right)\right] - 3C_{11}\right\} r^{\nu_{2m}-3/2}$$

$$\sigma_{r_1\theta_1}(xz) = \sigma_{r_1\phi_1}(xz) = \sigma_{\theta_1\phi_1}(xz) = 0 \tag{4}$$

As can be expected from the axially symmetric nature of the applied load about the y axis, all the stress components are independent of angular coordinates. Thus, the spherulite is, in effect, in a state of two-dimensional hydrostatic tension in the xz plane.

In a similar manner, the corresponding strains in the xz plane are found to be

$$e_{r_1}(xz) = 2A_{01}K_{01}\left(\nu_{01} - \frac{1}{2}\right) r^{\nu_{01}-3/2} + \frac{1}{2}\sum_{m=1,3} A_{2m}K_{2m}\left(\nu_{2m} - \frac{1}{2}\right) r^{\nu_{2m}-3/2}$$

$$e_{\theta_1}(xz) = 2A_{01}K_{01}r^{\nu_{01}-3/2} + \frac{1}{2}\sum_{m=1,3} A_{2m}K_{2m}r^{\nu_{2m}-3/2}$$

$$e_{\phi_1}(xz) = 2A_{01}K_{01}r^{\nu_{01}-3/2} + \sum_{m=1,3} A_{2m}\left(\frac{1}{2}K_{2m} - 3\right) r^{\nu_{2m}-3/2}$$

$$e_{r_1\theta_1}(xz) = e_{r_1\phi_1}(xz) = e_{\theta_1\phi_1}(xz) = 0 \tag{5}$$

Also of interest here are the stresses and strains along the y axis, which can be found by setting $\phi_1 = \phi_2 = \pi/2$

and $\theta_1 = \theta_2 = \pi/2$ in eqs 1–3. Thus

$$\sigma_{r_1}(y) = 2A_{01}K_{01}\left[C_{33}\left(\nu_{01} - \frac{1}{2}\right) + 2C_{13}\right]r^{\nu_{01}-3/2} - \sum_{m=1,3} A_{2m}\left[C_{33}K_{2m}\left(\nu_{2m} - \frac{1}{2}\right) + 2C_{13}(K_{2m} - 3)\right]r^{\nu_{2m}-3/2}$$

$$\sigma_{\theta_1}(y) = \sigma_{\phi_1}(y) = 2A_{01}K_{01}\left[C_{11} + C_{12} + C_{13}\left(\nu_{01} - \frac{1}{2}\right)\right]r^{\nu_{01}-3/2} + \sum_{m=1,3} A_{2m}\left\{-K_{2m}\left[C_{11} + C_{12} + C_{13}\left(\nu_{2m} - \frac{1}{2}\right)\right] + 3(C_{11} + C_{12})\right\}r^{\nu_{2m}-3/2}$$

$$\sigma_{r_1\theta_1}(y) = \sigma_{r_1\phi_1}(y) = \sigma_{\theta_1\phi_1}(y) = 0 \tag{6}$$

$$e_{r_1}(y) = 2A_{01}K_{01}\left(\nu_{01} - \frac{1}{2}\right)r^{\nu_{01}-3/2} - \sum_{m=1,3} A_{2m}K_{2m}\left(\nu_{2m} - \frac{1}{2}\right)r^{\nu_{2m}-3/2}$$

$$e_{\theta_1}(y) = e_{\phi_1}(y) = 2A_{01}K_{01}r^{\nu_{01}-3/2} + \sum_{m=1,3} A_{2m}(3 - K_{2m})r^{\nu_{2m}-3/2}$$

$$e_{r_1\theta_1}(y) = e_{r_1\phi_1}(y) = e_{\theta_1\phi_1}(y) = 0 \tag{7}$$

Since the exponents ν_{01}, ν_{21}, and ν_{23} of the radius r are functions of elastic moduli of the anisotropic spherulite, we can expect both the stress and strain distributions to be nonuniform under biaxial tension.[1] Moreover, as we noted in an earlier publication,[1] the presence of ν_{23} ($\nu_{23} \leq 3/2$) in eqs 4–7 gives rise to stress (or strain) singularities at the center of the spherulite. This is to be contrasted with the case of hydrostatic (triaxial) compression or tension which results in nonuniform but otherwise finite stresses and strains in the spherulite.[1] The fact that the stresses are bounded in triaxial tension (or compression) but unbounded in biaxial and uniaxial tensions suggests that the behavior of the spherulite is sensitive to the symmetric nature of the applied load.

The physical basis for this sensitivity to load symmetry is not immediately clear, but it is probably associated with the spherically symmetric structure of the spherulite. Since the structure is in essence an aggregate of many identical cone elements, the elements should be able to share the applied load evenly under a spherically symmetrical hydrostatic tension or compression. In fact, the analytical results of the previous study[1] show that this hydrostatic load induces only normal stresses (i.e., radial and hoop) in each cone element, and all stresses diminish to zero as one approaches the origin of the spherulite.

Pure Shear

We now turn to the case of pure shear, which, as mentioned before, is equivalent to subjecting the polymer to a pair of mutually orthogonal loads, T, in which one load (say, the one along the z axis) is tensile and the other (along the x axis) is compressive. We will again consider only those stress and strain components that are of significance in this case. These include the principal shear stress τ and principal shear strain γ, which are given by

Table I
Elastic Constants of Bulk Polyethylene and Polyethylene Spherulite at 70% Crystallinity and 20 °C[a]

bulk polyethylene	
Young's modulus × 10^{10} dyn/cm^2	2.05
Poisson's ratio	0.459
polyethylene spherulite	
$C_{11} \times 10^{10}$ dyn/cm^2	14.87
$C_{33} \times 10^{10}$ dyn/cm^2	4.61
$C_{12} \times 10^{10}$ dyn/cm^2	13.77
$C_{13} \times 10^{10}$ dyn/cm^2	4.69
$C_{44} \times 10^{10}$ dyn/cm^2	0.46

[a] Data of Wang.[7]

$$\tau = \frac{1}{2}(\sigma_{\theta_1} - \sigma_{\phi_1}) = \frac{3}{2}(C_{11} - C_{12})(\sin^2\theta_2 - \sin^2\theta_2 \cos 2\chi)\sum_{m=1,3} A_{2m}r^{\nu_{2m}-3/2} \tag{8}$$

$$\gamma = (e_{\theta_1} - e_{\phi_1}) = 3(\sin^2\theta_1 - \sin^2\theta_2 \cos 2\chi)\sum_{m=1,3} A_{2m}r^{\nu_{2m}-3/2} \tag{9}$$

It may be noted that γ is the engineering principal shear strain which is twice its tensorial counterpart.

From eqs 8 and 9, both τ and γ are seen to reach maximum at $\theta_1 = \theta_2 = \pm\pi/2$ and $\chi = \pi/2$ and $3\pi/2$ (i.e., along the y axis) for any given radius. Consequently,

$$\tau(\max) = 3(C_{11} - C_{12})\sum_{m=1,3} A_{2m}r^{\nu_{2m}-3/2} \tag{10}$$

$$\gamma(\max) = 6\sum_{m=1,3} A_{2m}r^{\nu_{2m}-3/2} \tag{11}$$

The other major stress and strain components are the radial stress σ_{r_1} and strain e_{r_1} along the z axis ($\theta_1 = 0$, $\theta_2 = \pi/2$, $\phi_2 = 0$, $\chi = \pi$) and the hoop stress σ_{θ_1} and strain e_{θ_1} along the x axis ($\theta_1 = \pi/2$, $\theta_2 = 0$, $\phi_1 = 0$, $\chi = \pi$).

$$\sigma_{r_1}(z) = \frac{3}{2}\sum_{m=1,3} A_{2m}\left[C_{33}K_{2m}\left(\nu_{2m} - \frac{1}{2}\right) + 2C_{13}(K_{2m} - 3)\right]r^{\nu_{2m}-3/2} \tag{12}$$

$$e_{r_1}(z) = \frac{3}{2}\sum_{m=1,3} A_{2m}K_{2m}\left(\nu_{2m} - \frac{1}{2}\right)r^{\nu_{2m}-3/2} \tag{13}$$

$$\sigma_{\theta_1}(x) = -\frac{3}{2}\sum_{m=1,3} A_{2m}\left\{K_{2m}\left[C_{11} + C_{12} + C_{13}\left(\nu_{2m} - \frac{1}{2}\right)\right] - 2(2C_{11} + C_{12})\right\}r^{\nu_{2m}-3/2} \tag{14}$$

$$e_{\theta_1}(x) = -\frac{3}{2}\sum_{m=1,3} A_{2m}(K_{2m} - 4)r^{\nu_{2m}-3/2} \tag{15}$$

An interesting feature in the above solutions is the presence of either $r^{\nu_{21}-3/2}$ or $r^{\nu_{23}-3/2}$ in each term. By comparison, the solutions for the hydrostatic tension or compression[1] contain only terms with $r^{\nu_{01}-3/2}$. (For that matter, the solutions to uniaxial and biaxial tensions are seen to contain terms with $r^{\nu_{01}-3/2}$ and $r^{\nu_{21}-3/2}$ or $r^{\nu_{23}-3/2}$.) Since both ν_{01} and ν_{2m} ($m = 1, 3$) are basically the elastic constants of the spherulite, it may be inferred that the

exponent ν_{01} is associated with the bulk responses while ν_{21} and ν_{23} are related to the shear behavior of the spherulite. Furthermore, as ν_{23} is the only exponent that gives rise to stress singularity,[1] it would seem that the singular behavior occurs only when the applied load is such that it induces shear stresses or strains in the radial cone sectors of the spherulite, e.g., $\sigma_{r_1\theta_1}$ and $\sigma_{r_1\phi_1}$ (or $e_{r_1\theta_1}$ and $e_{r_1\phi_1}$). This is in keeping with the statement we made in the previous section since all the applied loads that are not spherically symmetrical (e.g., uniaxial and biaxial tensions, and pure shear) are apt to generate such stresses.

From eq A-2 and 3, we can show that the radial strain, e_{r_1}, along the y axis is zero. This is in agreement with the physical reality that in pure shear, there should be no strain in the direction normal to the plane of loading.

Numerical Example

In order to have a more quantitative understanding of the results obtained above, we consider in this section a numerical example pertaining to biaxial tension and pure shear in the spherulitic polyethylene. To this end, we assume the sample to be 70% crystalline and to have a set of elastic moduli whose values are listed in Table I.[1,7]

Results for biaxial tension are shown in Figure 2 where both the stress and strain components, normalized with respect to the corresponding quantities at distant field, are plotted as functions of r/a, a being the outer radius of the spherulite. For the sake of clarity, the subscript 1 has been omitted from all quantities in Figure 2 and subsequent figures. A point of particular interest in the plot is the distributions of stress and strain around the origin of the spherulite. While these distributions are seen to rise rapidly toward the center, the rise is much more limited to the immediate neighborhood of the center when compared with the results for uniaxial tension; thus the center region of the spherulite should be more susceptible to localized yielding or fracture in biaxial tension. This prediction is well borne out by the experiments of Haas and McRae[9,10] and Tanaka et al.,[11] who found consistent development of highly localized yield zones or cracks at spherulite centers when they subjected films of polyethylene, polybutene-1, and polypropylene to biaxial tension. By comparison, samples subjected to simple tension have been found to develop extensive yield zone covering both the center and equatorial regions of the spherulite.[3-6,12]

A further point of interest in Figure 2 is the large concentration of hoop stresses σ_{θ_1} and σ_{ϕ_1} at the outer radius $r = a$ on the y axis, i.e., at the points $(0, \pm y_1, 0)$ in Figure 1. Their normalized value, or stress concentration factor, is 4.24, which is to be compared with the corresponding value of 2.5 for simple tension (cf. Figure 1 ref 1). However, the effect of this stress concentration should be difficult to observe under microscope since, when projected on the xz plane, the concentration sites coincide with the spherulite center where an even greater stress concentration exists.

In Figure 3, we show how the overall shape of the spherulite and its concentric shells would look in the yz and xz planes when the bulk sample is subjected to a biaxial load. To obtain these results, we chose a load of 0.5×10^{10} dyn/cm^2 and calculated the dimensional changes using the displacements described in Appendix 2. The load used in this calculation is apparently excessive, as can be seen from the resulting deformation which is well beyond the limit allowed in the linear theory of elasticity.[2,8] Thus the results should be regarded as only semiquantitative.

As seen in Figure 3, the deformation is different in each shell; in the xz plane, for example, the innermost shell

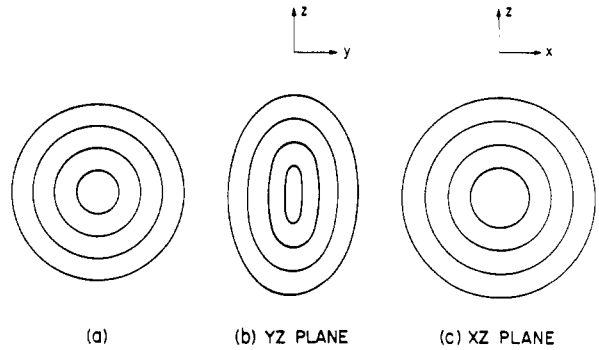

Figure 3. Sketch of the spherulite and its concentric shells before (a) and after (b and c) the polymer has been subjected to a biaxial load of 0.5×10^{10} dyn/cm^2.

undergoes a dimensional change of about 38% while the outermost shell experiences a change of only about 13%. We note, however, that these predictions are less apparent in the microscopic observations of Haas and McRae[9,10] and Tanaka et al.[11] because their photomicrographs were obtained from samples that had already undergone appreciable yielding or fracture at the spherulite centers. Consequently, the large deformation gradient along the radius, which is predicted to occur in our elastic analysis, may have been relieved substantially by the yielding or fracture.

The corresponding results for the case of pure shear (with $T = 0.25 \times 10^{10}$ dyn/cm^2) are shown in Figures 4 and 5. The displacement field for pure shear is given in Appendix 3. In comparison with the results of biaxial tension, the stress distribution around the spherulite center tends to be more diffused; furthermore, there is a large buildup of hoop stress σ_{θ_1} at the outer radius, $r = a$, on the x axis. Consequently, in addition to the primary zone at the spherulite center, a secondary yield zone is expected to develop in the plane of shear (xz plane), 45° away from the shear axis. This is in qualitative agreement with the experimental results of polybutene-1 obtained by Boni et al.[13] (cf. Figure 9 of ref 13).

In the work of Boni et al.[13] it is also reported that the cross-sectional area of their polybutene-1 spherulite increased upon shear. This result is at variance with our prediction which shows very little change in the cross-sectional area in the example treated in Figure 5. As pointed out by Boni et al.,[13] their experiment had been seriously affected by the problem associated with thinness and short gage length of the film sample. The former causes the film to buckle while the latter induces additional strains from the gripping area. Accordingly, their quantitative data remain to be confirmed by additional experiment.

A remark should be made in regard to the experimental data quoted in this paper. Since microscopic observation of the spherulite deformation requires the specimens to be as thin as possible, the spherulites under observation may be in a truncated form rather than in spherical shape.[14] This should not significantly affect our analytical results, however, since the major predictions, e.g., stress singularities and inhomogeneous deformations, are associated with the spherically symmetrical structure (or spherical isotropy) of the spherulite and not with its shape. On the other hand, if the thickness of the specimen is much less than the diameters of the spherulites, the analysis may require some modification. This problem will be dealt with in a future publication.

Summary

The spherulites are found to undergo highly inhomogeneous deformation when the polymer is subjected to

biaxial tension or pure shear. This deformation is accompanied by stresses whose distributions are even more nonuniform and tend to infinity at the spherulite centers. However, while similar results are also observed in simple tension, the region of high stresses is especially much more localized in biaxial tension than in other loadings. The results are found to be qualitatively in agreement with experimental data reported in the literature.

Appendix 1. Displacements, Strains, and Stresses in the Spherulite when the Polymer Is Subjected to Simple Tension

Displacements:

$$u_r = A_{01}K_{01}r^{\nu_{01}-1/2} + \frac{1}{4}(1 + 3\cos 2\theta)\sum_{m=1,3} A_{2m}K_{2m}r^{\nu_{2m}-1/2}$$

$$u_\theta = -\frac{3}{2}\sin 2\theta \sum_{m=1,3} A_{2m}r^{\nu_{2m}-1/2}$$

$$u_\phi = 0 \qquad \text{(A-1)}$$

Strains:

$$e_r = A_{01}K_{01}\left(\nu_{01} - \frac{1}{2}\right)r^{\nu_{01}-3/2} + \frac{1}{4}(1 + 3\cos 2\theta)\sum_{m=1,3} A_{2m}K_{2m}\left(\nu_{2m} - \frac{1}{2}\right)r^{\nu_{2m}-3/2}$$

$$e_\theta = A_{01}K_{01}\left(\nu_{01} - \frac{1}{2}\right)r^{\nu_{01}-3/2} + \sum_{m=1,3} A_{2m}[K_{2m}(1 + 3\cos 2\theta)/4 - 3\cos 2\theta]r^{\nu_{2m}-3/2}$$

$$e_\phi = A_{01}K_{01}\left(\nu_{01} - \frac{1}{2}\right)r^{\nu_{01}-3/2} + \sum_{m=1,3} A_{2m}[K_{2m}(1 + 3\cos 2\theta)/4 - 3\cos^2\theta]r^{\nu_{2m}-3/2}$$

$$\gamma_{r\theta} = -\frac{3}{2}\sin 2\theta \sum_{m=1,3} A_{2m}\left(K_{2m} + \nu_{2m} - \frac{3}{2}\right)r^{\nu_{2m}-3/2}$$

$$\gamma_{r\phi} = \gamma_{\theta\phi} = 0 \qquad \text{(A-2)}$$

Stresses:

$$\sigma_r = C_{13}(e_\theta + e_\phi) + C_{33}e_r$$

$$\sigma_\theta = C_{11}e_\theta + C_{12}e_\phi + C_{13}e_r$$

$$\sigma_\phi = C_{12}e_\theta + C_{11}e_\phi + C_{13}e_r$$

$$\sigma_{r\theta} = C_{44}\gamma_{r\theta} \qquad \text{(A-3)}$$

Here the polar axis is in the direction of applied tension T and c_{ij} are elastic constants of the spherulite. The subscripts 1, 2, 3, and 4 are identified respectively with the axis pairs, $\theta\theta$, $\phi\phi$, rr, and $r\theta$ or $r\phi$. Also, the symbols

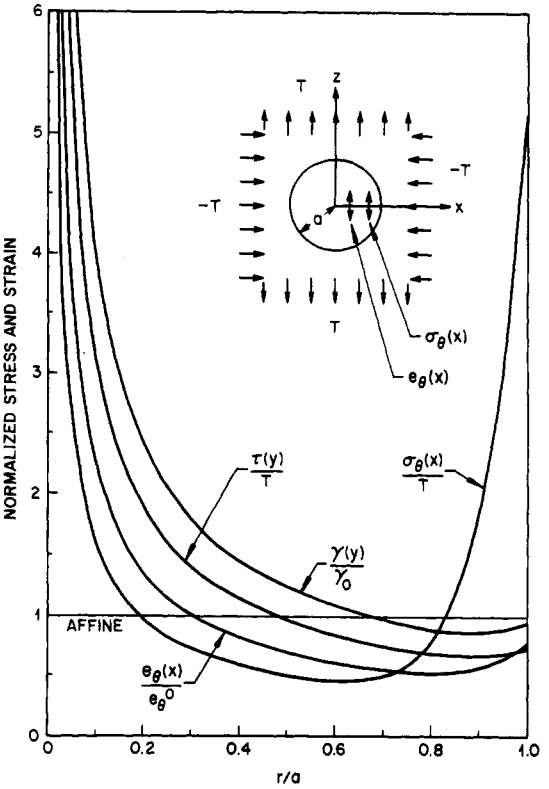

Figure 4. Distributions of major stresses and strains in the spherulite when the polymer is subjected to pure shear in the xz plane. Both stresses and strains have been normalized with the corresponding quantities at distant field and the radius, r, has been normalized with the outer radius, a, of the spherulite.

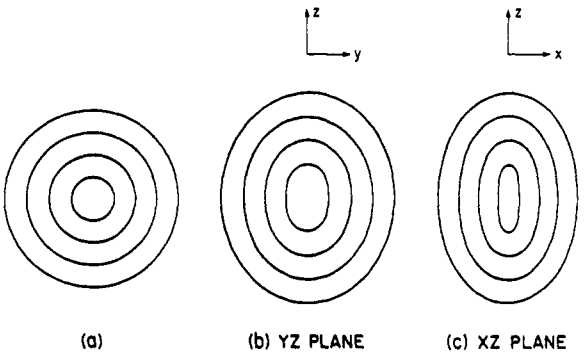

Figure 5. Sketch of the spherulite with its concentric shells before (a) and after (b and c) the polymer has been subjected to a shear load of 0.25×10^{10} dyn/cm^2.

ν_{01}, ν_{21}, ν_{23}, K_{01}, K_{21}, and K_{23} are defined as[7]

$$\nu_{01} = \left[1/4 + \frac{2(C_{11} + C_{12} - C_{13})}{C_{33}}\right]^{1/2} \qquad \text{(A-4)}$$

$$K_{01} = \frac{(2C_{44} + C_{12} - C_{11}) - C_{44}(\nu_{01}^2 - 1/4)}{(C_{13} + C_{44})(\nu_{01} - 1/2) + (2C_{44} + C_{12} + C_{11})} \qquad \text{(A-5)}$$

$$\nu_{21} = [a_2 + (a_2^2 - b_2)^{1/2}]^{1/2} \qquad \text{(A-6)}$$

$$\nu_{23} = [a_2 - (a_2^2 - b_2)^{1/2}]^{1/2} \qquad \text{(A-7)}$$

$$K_{2m} = \frac{5C_{11} + C_{12} - C_{44}(\nu_{2m}^2 - 9/4)}{(C_{13} + C_{44})(\nu_{2m} - 1/2) + (2C_{44} + C_{11} + C_{12})} \qquad m = 1, 3 \qquad \text{(A-8)}$$

where

$$2C_{33}C_{44}a_2 = 6[C_{44}^2 + C_{11}C_{33} - (C_{13} + C_{44})^2] + C_{33}(2C_{44} + C_{12} - C_{11}) + 2C_{44}(C_{11} + C_{12} - C_{13}) + 1/2C_{33}C_{44} \quad \text{(A-9)}$$

$$C_{33}C_{44}b_2 = [6C_{44} + 2(C_{11} + C_{12} - C_{13}) + 1/4C_{33}][6C_{11} + 2C_{44} + C_{12} - C_{11} + 1/4C_{14}] - 6[2C_{44} + C_{12} + C_{11} - 1/2(C_{13} + C_{44})]^2 \quad \text{(A-10)}$$

The integration constants are obtained by requiring that the displacements in the spherulite and the matrix be continuous at the interface $r = a$ and that the materials be in mechanical equilibrium at the interface. Thus,

$$A_{21}a^{\nu_{21}-3/2} = \frac{5(1-\nu)T}{2(4-5\nu)D}[2C_{44}(K_{23} + \nu_{23} - 3/2) - C_{33}K_{23}(\nu_{23} - 1/2) - 2C_{13}(K_{23} - 3) - 8G(K_{23} - 2)] \quad \text{(A-11)}$$

$$A_{23}a^{\nu_{23}-3/2} = \frac{-5(1-\nu)T}{2(4-5\nu)D}[2C_{44}(K_{21} + \nu_{21} - 3/2) - C_{33}K_{21}(\nu_{21} - 1/2) - 2C_{13}(K_{21} - 3) - 8G(K_{21} - 2)] \quad \text{(A-12)}$$

$$A_{01}K_{01}(3K + 4G)a^{\nu_{01}-3/2} = \frac{3(7-5\nu)(1-\nu)T}{4(4-5\nu)(1+\nu)} - \sum_{m=1,3} A_{2m}a^{\nu_{2m}-3/2}\left[1/4C_{33}K_{2m}(\nu_{2m} - 1/2) + 1/2C_{13}(K_{2m} - 3) + 3G\frac{(7\nu - 5)}{(8-10\nu)} + K_{2m}G\frac{(11-13\nu)}{(8-10\nu)}\right] \quad \text{(A-13)}$$

G and ν are, respectively, the shear modulus and the Poisson's ratio of the bulk sample, which is assumed to be isotropic. Also

$$D = \left\{C_{33}K_{21}(\nu_{21} - 1/2) + 2C_{13}(K_{21} - 3) + \frac{2G}{(4-5\nu)} \times [K_{21}(11-13\nu) - 3(5-7\nu)]\right\}\left\{C_{44}(K_{23} + \nu_{23} - 3/2) - \frac{G}{(4-5\nu)}[K_{23}(5-7\nu) - 17 + 19\nu]\right\} - \left\{C_{33}K_{23}(\nu_{23} - 1/2) + 2C_{13}(K_{23} - 3) + \frac{2G}{(4-5\nu)}[K_{23}(11-13\nu) - 3(5-7\nu)]\right\}\left\{C_{44}(K_{21} + \nu_{21} - 3/2) - \frac{G}{(4-5\nu)}[K_{21}(5-7\nu) - 17 + 19\nu]\right\} \quad \text{(A-14)}$$

Appendix 2. Displacements of the Spherulite in Biaxial Tension

In the yz plane:

$$u_{r_1} = 2A_{01}K_{01}r^{\nu_{01}-1/2} - (1 - 3\cos 2\theta_1)/4\sum_{m=1,3} A_{2m}K_{2m}r^{\nu_{2m}-1/2}$$

$$u_{\theta_1} = -\frac{3}{2}\sin 2\theta_1 \sum_{m=1,3} A_{2m}r^{\nu_{2m}-1/2} \quad \text{(A-15)}$$

In the xz plane:

$$u_{r_1} = 2A_{01}K_{01}r^{\nu_{01}-1/2} + \frac{1}{2}\sum_{m=1,3} A_{2m}K_{2m}r^{\nu_{2m}-1/2}$$

$$u_{\theta_1} = 0 \quad \text{(A-16)}$$

Appendix 3. Displacements of the Spherulite in Pure Shear

In the yz plane:

$$u_{r_1} = \frac{3}{4}(1 + \cos 2\theta_1)\sum_{m=1,3} A_{2m}K_{2m}r^{\nu_{2m}-1/2}$$

$$u_{\theta_1} = -\frac{3}{2}\sin 2\theta_1 \sum_{m=1,3} A_{2m}r^{\nu_{2m}-1/2} \quad \text{(A-17)}$$

In the xz plane:

$$u_{r_1} = \frac{3}{2}\cos 2\theta_1 \sum_{m=1,3} A_{2m}K_{2m}r^{\nu_{2m}-1/2}$$

$$u_{\theta_1} = -3\sin 2\theta_1 \sum_{m=1,3} A_{2m}r^{\nu_{2m}-1/2} \quad \text{(A-18)}$$

References and Notes

(1) Wang, T. T. *J. Polym. Sci., Phys. Ed.* **1974**, *12*, 145.
(2) De Saint-Venant, B. *J. Math. Pures Appl.* **1865**, Ser. 2, *8*, 297. Or see: Love, A. E. H. *The Mathematical Theory of Elasticity*, 4th ed.; Dover: New York, 1944; p 164.
(3) Adams, W. W.; Thomas, E. L. *Bull. Am. Phys. Soc.* **1980**, *25*, 251.
(4) Keith, H. D.; Padden, F. J. *J. Polym. Sci.* **1959**, *39*, 101.
(5) Fischer, E. W. *Z. Naturforsch.* **1957**, *A12*, 753.
(6) Geil, P. H. *Polymer Single Crystals* Interscience: New York, 1963; Chapters 4 and 5.
(7) Wang, T. T. *J. Appl. Phys.* **1973**, *44*, 4052.
(8) Timoshenko, S. P.; Goodier, J. N. *Theory of Elasticity*, 3rd ed.; McGraw-Hill: New York, 1971; p 10.
(9) Haas, T. W.; McRae, P. H. *SPE J.* **1968**, *24*, 27.
(10) Haas, T. W.; McRae, P. H. *Polym. Eng. Sci.* **1969**, *9*, 423.
(11) Tanaka, H.; Masuko, T.; Homma, K.; Okajima, S. *J. Polym. Sci., A-1* **1969**, *7*, 1977.
(12) Hay, I. L.; Keller, A. *Kolloid Z. Z. Polym.* **1965**, *204*, 43.
(13) Boni, S.; G'Sell, C.; Weynant, E.; Haudin, J. M. *Polym. Testing* **1982**, *3*, 3.
(14) Adams, W. W. Private communication.

Registry No. $(H_2C{=}CH_2)_x$ (homopolymer), 9002-88-4.